EnvironmentAsia
The international journal published by the Thai Society of Higher Education Institutes on Environment

Available online at www.tshe.org/EA
EnvironmentAsia 8(1) (2015) 101-114

Characteristics of Hailstorm over Northern Thailand during Summer Season

Pakdee Chantraket [a], Sukrit Kirtsaeng [b], Chanti Detyothin [b], Arisara Nakburee [a] and Kasem Mongkala [a]

[a] *Department of Royal Rain-making and Agricultural Aviation (DRRAA), Bangkok 10900, Thailand*
[b] *Meteorological Development Bureau, Thai Meteorology Department (TMD), Bangkok 10260, Thailand*

Abstract

This study focused on the potential parameters, as a result of the upper-air sounding with radiosonde and of the dual polarization radar for detecting hailstorms. The data were collected during the 2012 summer consisting of 12 hail and 1129 no-hail rainstorms of seven studied dates from April to May, 2012. They were analyzed to discern the character of hail and use them as data for detecting hail echoes and for severe weather forecast in upper Thailand. On the day of hail, the instability indices were high enough to contribute to its formation. The following indices include Lifted Index (LI), Showalter Index (SI) and Convective Available Potential Energy (CAPE). LI and SI displayed the marginally instability ranged -1 to -4. In the case of CAPE, it could reach the extreme instability (CAPE > 2500 J/kg) and also came with the large updraft speed.

TITAN software (Thunderstorm Identification, Tracking, Analysis and Nowcasting) was also applied for comparing rainstorms with hailstorms. The significant seven echo characteristics included storm period, speed, mean-maximum reflectivity in the horizontal polarization (ZH), area, volume and mass. Based on the character and frequency distributions in summer, hailstorms had greater values of storm duration, area, volume, mass, speed and highest reflectivity than individual rainstorms. Besides, the mean reflectivity of the storms was a negligible factor to identify the type of storm.

For the case study on hail by determining polarimetric radar measurement at S-band across Chiang Maun, Northern Thailand, radar signatures with EDGE software showed that the hail was detected 100% during its falling. It also presented as followings: Vertically integrated liquid (VIL) exceeding 100 kg/m^2, ZH over 60dBZ near the surface and ETOP greater than 17 km. Differential reflectivity (ZDR) of rain-hail mixtures almost reached zero. In addition, the coincidental values of correlation coefficient (CC) were ranged 0.988 and 0.996, and specific differential phase (KDP) was ranged 2.1 and 3.2 deg/km.

Keywords: hailstorm characteristics; TITAN; thunderstorms; dual polarization radar; radiosonde; Northern Thailand

1. Introduction

Formed by severe convective storms, hail stands as a natural risk. It can trigger great damages to human life, buildings. The amount of damage is dependent on the frequency and intensity of the hail as it falls. From a mesoscale point of view, hailstorm events are about atmospheric instability, strong updrafts and highly organized convective systems (Browning, 1977; Groenomeijer *et al*., 2007; Knight *et al*., 2001; Ragette, 1973; Robert, 2009). Normally during summer, there are the potentially strong updrafts (e.g. Johns *et al*., 1992; Miller *et al*., 1988; Nelson, 1987) in a thunderstorm, as well as the possibly high water vapor content of the atmosphere on a warm summer day. Therefore, the hail formed by a summer thunderstorm can reach fairly large diameters (Ludlam, 1980).

Hailstorms have been checked ever more by meteorological radar that permits precise analyses of storm tracks and spatial variability of hailfall. Several studies have been carried out to provide details on hailstorm creation and structure by radar. The weather radar relies on single-polarization or dual-polarization. The study of radar data-based hailstorm characteristics appears in the USA during the 1960s following the invention and first use of weather radars (Battan, 1963; Braham, 1958). Later, there have been many hailstorm studies using weather radar (e.g. Changnon, 1960; 1963; 1969; Towery *et al*., 1970). Changnon *et al*. (2009) has studied the behavior and characteristics of hail producing radar echoes that are sought as part of a comprehensive hail research program in Illinois. Waldvogel *et al*. (1979) has developed a real-time hail probability equation for 3-cm radars utilizing primarily the height of the 45dBZ echo above freezing level and developed a successful hail core aloft detection algorithm that uses output from WSR-88D storm analysis algorithms (Waldvogel *et al*., 1979; Witt, 1990). Hohl *et al*. (2002) has used radars to provide the near-ground information of hailfalls to detect hail in thunderstorms and count intensity of hailfall in Switzerland. Roxana *et al*. (2013) focuses on the

combined analysis of data recorded at ground and weather radar measure to assess the possible harmful hail.

In latest years, the new creation of dual-polarized weather radar schemes has been improved. It offers the opportunity to identify several classes of hydrometeors present in stratiform and convective storms (Bringi *et al*., 2001). It also detects significant signatures of hailstorm formation (e.g. Debin *et al*., 2010; Delobbe *et al*., 2003; Holler, 1994). This important feature depends on the fact that polarimetric radar measure is highly sensitive to physical properties of hydrometeors e.g. composition, size, shape and orientation (Vulpiani *et al*., 2005). Most technical writing about hydrometeor classification describes category techniques designed for S-band data (e.g. Lim *et al*., 2005; Straka *et al*., 2000; Vivekanandan *et al*., 1999; Zrnic *et al*., 2001). By now in Thailand, in spite of a few studies of hailstorms observed by radar, the related studies have been involved with radar-based convective storms performed by Chantraket *et al*. (2013). He investigates and classifies the two seasonal variations of rain storm character derived from Thunderstorm Identification and Tracking Analysis and Nowcasting (TITAN) (Dixon *et al*., 1993) over northern Thailand.

In Thailand, almost all hailstorms are related to summer thunderstorms and are small-scale phenomena often with short duration. During February through May, they rarely occur over the northeast and the north mainly in mountainous areas of the north. Normally, severe thunderstorms occur with hailstones reaching the ground in the afternoon. The hailstorms can cause large damage to buildings and crops and sometimes, human life as shown below in Fig. 1. For this reason, knowing the background of local hail and its nature is critical for the concept of its formative mechanism and signatures for advancing the hail forecast. Besides, the result provides the theory for further study on convective weather structures, and these characteristics lead to the basic progress in hail forecasting and suppression in Thailand.

This is to underline the study of hailstorm characteristics and find its signatures during summer over the North by analyzing meteorological states related to hail and non-hail events with radiosonde. The critical storm's properties, structures and behaviors are comparative between rainstorms and hailstorms (Towery *et al*., 1970). The case study of hail is exposed by the significant radar properties derived from dual polarization radar. Radar and the upper-air sounding are obtained from the weather station of DRRAA, Omkoi District, Chiang Mai. The storm characteristics are run through TITAN and EDGE (Enterprise Doppler Graphic Environment) software. Standard instability indices are computed with the upper-air sounding data. These instrumentations can provide an efficient way to study

Figure 1. Strong wind shear by hailstorm and damages by small hail in Chiang Maun District, Phayao Province, Northern Thailand on 27 April 2012, 1000UTC

and observe the storm's nature as well as its essential features.

2. Data sets and Methodology

Hail records: The following data were 12 hail-events (cells) of 7-day samples during the 2012 summer. They include 4 days (8 events) in April 2012 and 3 days (4 events) in May 2012. All facts were based on the report of hail observatory volunteers that they performed with radar effective radius 240 km in the North. Still, the no-hail events were chosen from severe convective rainstorm (after this called rainstorm) at the same period as the 12 hail events occurred. As the event numbers differed in each sampled day, these data were then analyzed to express characteristics of storm and to provide critical information for detecting and forecasting hail-producing echoes. The hail events and their place are shown as in Table 1 and Fig. 2.

Radar data has the advantage of high spatial and temporal resolutions, resulting in a very feasible option to detect hail in combination with an operational weather station. The extra data sets included hailstorm and rainstorm characteristics taken from radar reflectivity measure, instability indices. They also needed meteorological factors computed by radiosonde watching. These data were compiled in only one day utilizing the observed hail, radar and sounding.

RADAR: The study used parameters derived from the reflectivity of S-band Doppler Radar with dual polarization (SIDPOL). Operated by DRRAA, SIDPOL is installed in Omkoi District, Chiangmai, and northern Thailand as shown in Fig. 2. The radar with EDGE™ software collected the reflectivity data as volume scan to the highest altitude up to 20 km provided in the universal format files (UF) (Barnes, 1980). The files were obtained every 6-minute interval by using 8 elevation angles. The main features are shown in Table 2.

Table 1. Observation of hail and no-hail events in northern Thailand during April- May 2012

Hail events (HS: Hailstorm)	Time (Local)	Time (UTC)	Latitude	Longitude	Place	Synoptic situation
(1) 20-Apr-12: Hail =1 event, No-hail=90 events						
HS#1	16:00	9:00	18.5681	100.1240	-Phrae (Song)	Heat low, Southerly wind and hot to very hot during the day
(2) 24-Apr-12: Hail =1 event, No-hail=60 events						
HS#1	18:00	11:00	16.8868	99.6783	-Sukhothai (Khiri Mat)	Low pressure, Southerly winds and hot to very hot during the day
(3) 27-Apr-12: Hail =4 event, No-hail=115 events						
HS #1	13:42	6:42	18.8903	100.2794	-Phayao (Chiang Muan) -Phrae (Song) -Lampang (Mae Mo) -Nan (Ban Laung)	High pressure and hot to very hot during the day
HS #2	15:06	8:06	19.4632	97.9334	-Mae Hong Son (Mueang)	
HS #3	17:18	10:08	19.0057	100.2040	-Phayao (Chiang Muan)	
HS #4	19:06	12:06	18.5008	100.4116	-Phrae (Song) -Lampang (Mae Mo)	
(4) 28-Apr-12: Hail =2 events, No-hail= 54 events						
HS #1	16:12	9:12	19.3713	99.8112	-Phayao (Mae Chai)	Heat low, high pressure and hot to very hot during the day
HS #2	15:00	8:00	19.5302	99.5768	-Chiang Rai (Mae Suai)	
(5) 2-May-12: Hail =1 event, No-hail= 198 events						
HS #1	17:54	10:54	17.0025	99.7100	-Sukhothai (Mueang)	Westerly winds
(6) 3-May-12: Hail =1 event, No-hail= 280 events						
HS #1	13:54	6:54	18.7805	99.8341	-Lampang (Nhao)	Heat low and hot to very hot during the day
(7) 4-May-12: Hail =2 events, No-hail= 332 events						
HS #1	15:12	8:12	19.1069	99.0740	-Chiang Mai (Mae Taeng)	Heat low and Southwesterly winds
HS #2	18:12	11:12	18.2334	99.9497	-Phrae (Long)	

Table 2. Main features of Omkoi radar, Chiang Mai, Thailand

Feature	Omkoi radar
Frequency	S Band (2800 MHz) / Wavelength 10.7 cm
Peak power	850 kW
Beamwidth	1.2°
Pulse width	0.8 μs
PRF	560 Hz
Range	240 km
Gate width	250 m
Volume scan (8 elevation angles)	0.5°, 1.45°, 2.2° 3.1°, 4.5°, 5.6°, 7.8° and 9.0°

TITAN: SIDPOL data in horizontal polarization (ZH) were run through TITAN as referred to Dixon *et al*. (1993). TITAN algorithm objectively identifies storms, tracks their movement and analyzes their 7 properties including (1) storm period (hours), (2) mean volume (km^3), (3) mean mass (kTons), (4) mean envelope area (km^2), (5) mean storm-top height (km MSL), (6) mean and maximum ZH (dBZ) and (7) mean speed (km/hr). Both of rainstorms and hailstorms were selected the dataset from the following criteria: (Chantraket *et al*., 2013; Dixon, 1998)

1) Storm track with radar effective radius 240 km
2) Reflectivity threshold at 30dBZ or greater
3) Minimum storm size as 10 km^2
4) Storm mass computed by the Z-M relationship; $m=20300*Z^{1.67}$, where m is the water content (in g/m^3) and Z is the radar reflectivity factor (in mm^6/m^3)

SOUNDING DATA: The upper-air soundings are regularly taken at the Royal Rain-Making meteorological station, Omkoi, Chiang Mai, Thailand (Fig. 2) from summer lasting late rainy season every year. The observed elements included stability indices, meteorological parameters as 4-level of relative humidity and wind properties as 4-level of wind speed and wind shear within Omkoi domain for each day. The indices and essential parameters were determined for the 00UTC sounding.

3. Result and Discussion

3.1. Meteorological situation relevant to hail and non-hail events

The study presented significant values of parameters derived from radiosonde for severe weather forecast concerning convective storms. The 19 parameters were obtained from the 00UTC soundings in Omkoi. Besides, 43 radiosonde data from April

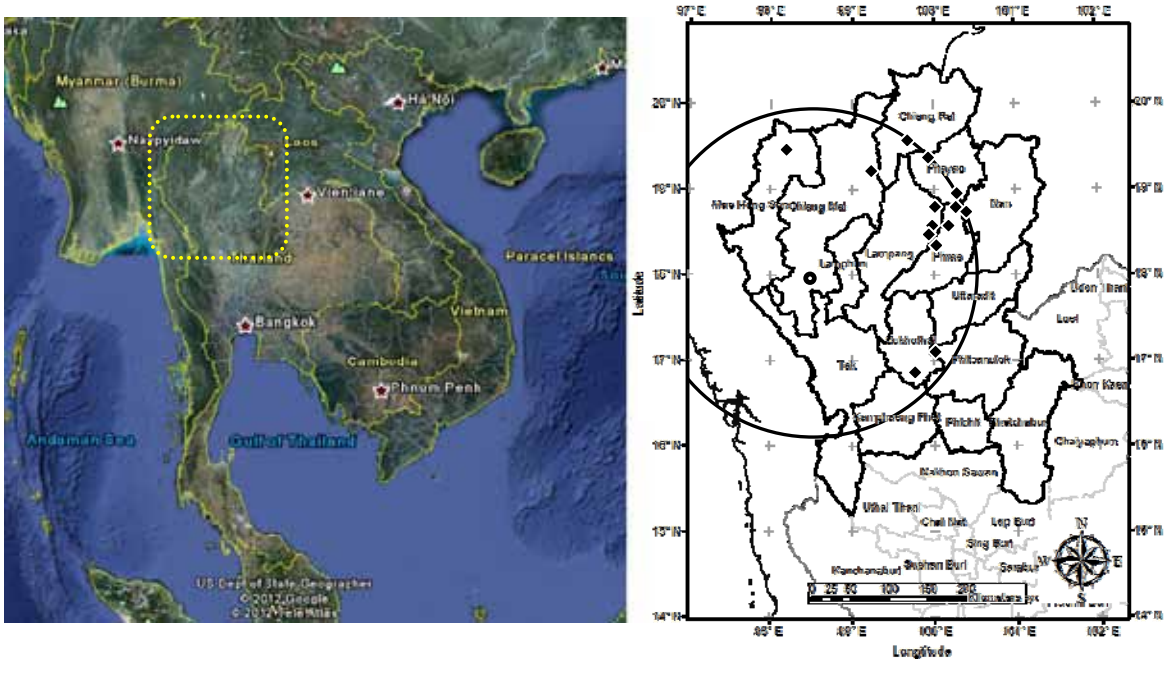

Figure 2. Study area, Omkoi radar station (18 47 54 N, 98 25 56 E, 1163 m MSL) effective range 240 km over northern Thailand and location of hail observation (black diamond) during 7 days in summer.

(20 days) to May 2012 (23 days) included independent 36 days for non-hail events and 7 days for hail. The significant parameters consisted of 8 parameters for instability indices (Robert, 2009; Brimelow *et al*., 2002): Precipitation Water (PW), Lifted Index (LI), Showalter Index (SI), Total of Totals Index (TTI), K Index (KI), Convective available potential energy (CAPE), Convective inhibition (CIN), and Severe Weather Threat Index (SWEAT). Also, 10 parameters for extra meteorological data included: freezing level (Xie *et al*., 2010), 4-averaged level relative humidity (RH), 4-averaged wind speed and wind shear from surface to 6 km, respectively. The parameters were valued in Table 3 and the skew-T diagram shown in Fig. 3.

From Table 3, the Radiosonde parameters in the thermodynamic analysis were selected where hail exceeded the mean value (in bold face) of non-hail occurrences all in hail events from April to May 2012. It is apparently that high indices are conducive for hail storm progress displaying values of LI (Celsius), SI (Celsius) and CAPE (J/kg), respectively. According to previous studies, the result confirms those of (e.g. Ceperuelo *et al*., 2006; Geoenemeijer *et al*., 2007; Robert, 2009). They showed the relation among hailstorms, LI and CAPE in the United States and The Netherlands. More, Sanchez *et al*. (2009) found SI parameter suitable to hail forecast in Spain.

From Table 3, the high instability was detected in the thermodynamic analysis where the hail exceeded the mean value (in bold face) from April to May 2012. High indices are conducive for hail storm progress displaying values of LI (Celsius), SI (Celsius) and CAPE (J/kg), respectively. According to previous studies, the result confirms those of (e.g. Ceperuelo *et al*., 2006; Geoenemeijer *et al*., 2007; Robert, 2009). They showed the relation among hailstorms, LI and CAPE in the United States and The Netherlands. More, Sanchez *et al*. (2009) found SI parameter suitable to hail forecast in Spain.

In both months, hail occurred with high CAPE reaching up to the extreme instability; CAPE > 2500 J/kg which also related the large updraft speed as mention to Doswell *et al*. (1977). In other words, the storms grew quick and vertical. At the same time, hail possibly increased due to both updraft strength and CAPE rise. Both LI and SI expressed the marginal instability (-1 to -4) and distinguished the events of April and May. In comparison, the more negative LI and SI in April, the stronger convective updraft and the more unstable troposphere in April were higher than May. For now, the rest parameters including PW, TTI, KI, CIN, SWEAT and the other meteorological data from sounding (Table 3) exhibited the overlapping values between rainstorms and severe storms. It slightly distinguishes the environment of hail from non-hail occurrences, but further studies with these parameters are necessary for more investigation.

3.2. Comparison of rainstorm and hailstorm

The importance of all 7 different radar properties (e.g. Chantraket *et al*., 2013; Towery, 1970) was calculated by TITAN, including: (1) the storm duration (hour), (2) the mean volume (km^3), (3) the mean mass (kTon), (4) the mean envelope area (km^2), (5) the maximum height of the storm-peak (km MSL), (6) the mean and maximum ZH (dBZ) and (7) the mean velocity (km/h). The analysis was performed for 7 days of hail events that occurred within the sweep of the

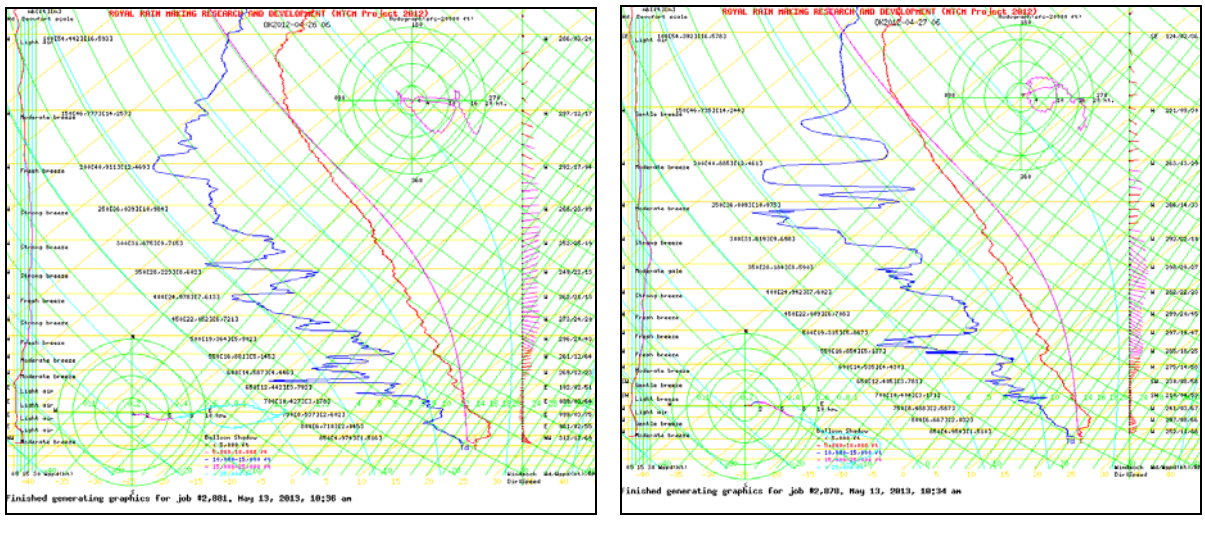

Figure 3. Skew-T diagram for non-hail (right) and hail (left) events on 26 April 2012, 0000UTC and 27 April 2012, 00UTC, respectively.

Table 3. Radiosonde parameters and dates of hail in April 2012 (20 days) to May 2012 (23 days)

Radiosonde Parameter	Non-hail occurrences	Hail occurrences				Non-hail occurrences	Hail occurrences		
	Mean value in April 2012	20-Apr-12	24-Apr-12	27-Apr-12	28-Apr-12	Mean value in May 2012	2-May-12	3-May-12	4-May-12
Precipitation Water SFC-850 (cm)	0.5	0.5	0.5	0.6	0.5	0.5	0.5	0.5	0.5
Lifted Index (^{o}C)	-2.1	**-3.2**	**-2.1**	**-3.0**	**-3.4**	-0.8	-1.5	-2.1	-2.3
Showalter Index	-0.9	**-2.7**	**-1.5**	**-2.8**	**-2.8**	-0.3	**-1.0**	**-1.2**	**-1.8**
Total of Totals Index	45.5	**47.6**	45.1	**46.6**	**47.5**	42.8	**44.1**	**44.8**	**45.7**
K Index	29.3	**32.8**	**31.2**	**32.5**	25.0	33.4	32.5	33.2	29.8
CAPE (J/kg)	3924.8	**5028.0**	**3930.0**	**5526.0**	**4786.0**	1225.7	**2918.0**	**4108.0**	**3827.0**
CIN (J/Kg)	-889.7	-873.0	**-992.0**	-677.0	-745.0	-697.2	-462.0	-501.0	-651.0
SWEAT Index	219.2	209.6	**246.6**	**248.0**	**246.6**	231.8	**242.0**	211.4	211.2
Freezing level (m)	4941	**5118**	**5042**	**5058**	**4942**	5168	4906	4835	5145
RH SFC -5 kft	73.1	**75.0**	**84.0**	**89.0**	**86.0**	88.4	84.0	78.0	80.0
RH 5 - 10 kft	52.7	**60.0**	**57.0**	**68.0**	**61.0**	75.8	72.0	63.0	62.0
RH 10 - 15 kft	39.9	**49.0**	**45.0**	**56.0**	**52.0**	68.6	58.0	62.0	52.0
RH 20 - 25 kft	21.6	11.0	20.0	**42.0**	**63.0**	61.0	60.0	41.0	56.0
Wind Speed SFC -5 kft (m/s)	6.1	**6.2**	5.1	5.1	4.1	4.8	**5.1**	**7.2**	**5.1**
Wind Speed 5 - 10 kft (m/s)	4.4	3.6	**5.1**	2.6	2.6	4.1	**4.6**	3.1	1.5
Wind Speed 10 - 15 kft (m/s)	5.15	3.6	**7.2**	4.1	**7.7**	3.6	**6.7**	3.1	2.1
Wind Speed 20 - 25 kft (m/s)	13.0	11.3	12.9	10.3	**14.4**	4.2	**7.2**	4.1	4.1
Wind shear SFC-6 km (m/s)	6.0	4.1	**7.2**	5.1	**7.7**	3.8	**6.7**	**5.6**	1.5

Note: bold face show the value of parameters exceeding the mean value in individual months.

Table 4. Comparison of radar reflection between hail and no-hail on dates of hailstorms

Storm Characteristics	No-hail* (1129 events)						Hail (12 events)					
	Mean	Min	Q1	Median	Q3	Max	Mean	Min	Q1	Median	Q3	Max
Mean Duration (hrs)	0.71±0.55	0.30	0.31	0.51	0.84	2.76	2.86±1.25	1.20	1.83	2.80	3.60	5.50
Mean Speed (km/hr)	8.70±7.86	0.09	2.17	6.40	14.24	32.85	17.45±8.93	1.51	12.95	17.12	23.23	29.82
Mean ZH (dBZ)	40.34±5.29	31.60	36.41	39.55	44.06	50.78	40.79±1.33	38.22	40.30	40.65	41.46	42.93
Maximum ZH (dBZ)	52.82±9.50	34.36	45.79	51.93	59.95	75.86	64.33±2.28	60.50	62.88	64.50	65.63	68.00
Mean Area (km^2)	26.13±29.86	5.60	10.63	15.80	26.87	221.33	180.76±44.62	116.64	152.77	170.42	221.00	258.26
Mean Volume (km^3)	87.70±123.98	15.58	24.56	43.67	94.47	945.72	762.62±193.18	530.07	602.63	758.83	880.83	1162.31
Mean mass (kTon)	61.40±100.80	5.36	19.08	32.36	53.43	744.43	798.32±251.80	446.58	574.25	783.77	895.37	1287.25
Maximum storm-top height (km)	5.33±2.04	2.09	3.70	4.88	6.83	9.27	8.56±1.03	6.38	7.88	9.00	9.38	9.38

* All cases of convective rainstorm at the same day which the 12 hail events occurred. Q1 and Q3 stand for Quartile 1 and Quartile 3, respectively.

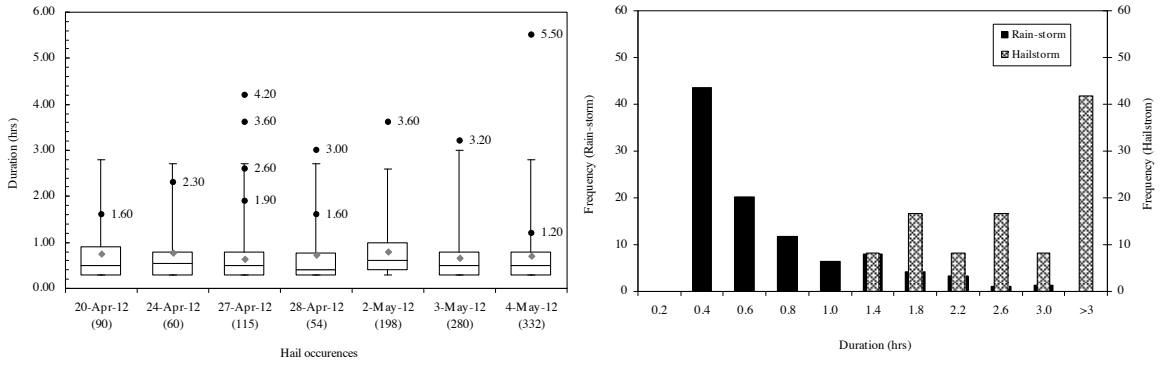

Figure 4. Box and whisker plot during rainstorms (left), number of individual rainstorm events each day (in brackets), average duration (gray dots), hail duration (black dots), and frequency distribution (right) during hailstorm.

radar loop. There were 12 incidents of hailstorm and also totally 1,129 incidents of rainstorm. As a result of preliminary analysis, the overall mean of hail storm events dominated the average individual rainstorms. The statistical analysis of all parameters is presented as Table 4.

3.2.1. Duration

The storm duration is considered the first reflection of radar beam at 30dBZ until the rainfall disappears. In this study, in comparison of the average individual storm with the hailstorm period, the longer lifetime the hailstorm has, the more frequent its long duration occurs (more than 3 hours). It implies that the hailstorm is often caused by the continuation of the multi-convective cell that is difficult to distinguish from the single-convective cell. The aspects of echo duration and the frequency distribution are reviewed as Fig. 4. The additional information is presented in Table 4. On the dates of hail, the mean duration of individual storms is less than 1 hour. Its highest period can vary up to 3 hours. Meanwhile, on the day of precipitation incidents, the hail period varies between 1.2 to 5.5 hours. It suggests that this range is greater than the mean duration of rainstorm of all events.

3.2.2. Speed

Tracks of all rainstorms were derived from radar analysis. The actual features of rainstorm's speed and the frequency distribution are shown as Fig. 5. The results indicated, in case of a rainstorm, the average speed of 9.0 km/hr and the greater frequency of about 10 km/hr. All together, it complied with the results obtained from Chantraket *et al*. (2013). He showed the mean speed of summer rainstorm 11 km/hr passing over the North of Thailand. Further, the result also explained that almost all of hailstorms showed the speed higher than the rainstorm's average speed, except for the reduced speed on 4 May 2012. This might be related to the long-duration of hailstorm and storm's speed which the further investigation is needed. The speed distribution of hail also revealed the greater frequency exceeding 20 to 30 km/hr.

3.2.3. Reflectivity

The radar analysis determined the threshold of storm's reflection from 30dBZ or more (Dixon, 1998). In addition, ZH average of rainstorm ranged between 35 to 46 dBZ. In comparison with hailstorms, they valued between 39 to 42dBZ. From Fig. 6, it should be noted that the mean ZH of storm was not considered

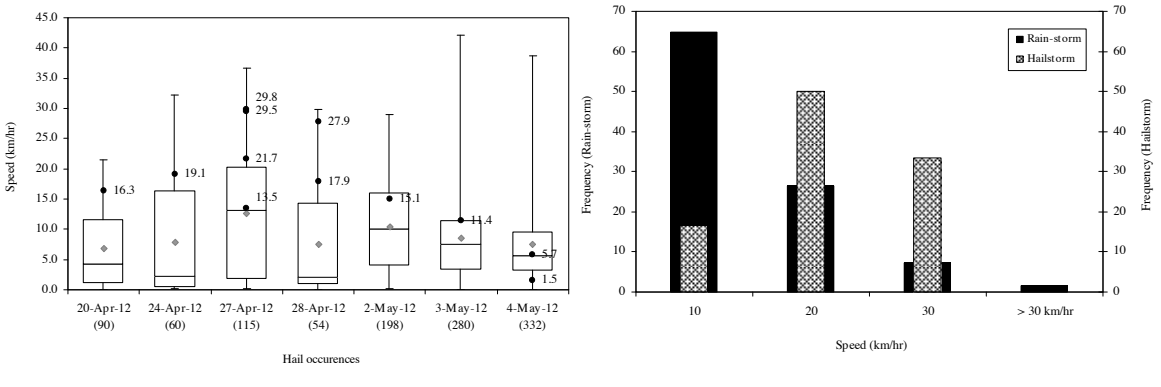

Figure 5. Box and whisker plot of rainstorm's speed (left), number of individual rainstorm events each day (in brackets), average speed (gray dots), hailstorm's speed (black dots), and frequency distribution (right) during hailstorm.

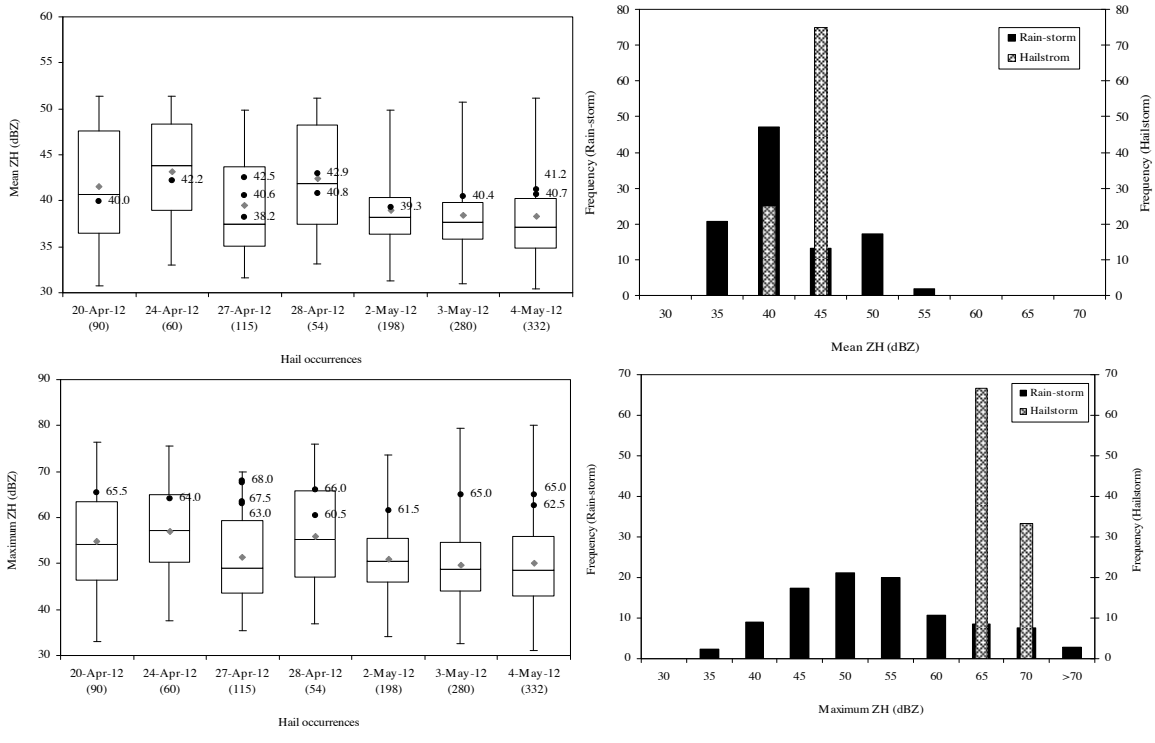

Figure 6. Box and whisker plot of storm's reflectivity (left), number of individual rainstorm events each day (in brackets), storm's reflectivity (gray dots), hailstorm's reflectivity (black dots), and frequency distribution (right) during hailstorm.

the right variables to identify the storm type. On the other hands, the ZH's maximum average dominated to identify between rainstorm and hailstorms. It was found that the ZH's maximum of all hail events was greater than of those rainstorms. Also, it determined several frequencies at higher 60dBZ.

3.2.4. Area, volume and mass

Radar analysis concerning storm's area, volume and mass decided the storm's size of more than 10 km^2 based on the threshold for the smallest storm's area (Dixon, 1998). The storm mass could be calculated by Z-M relations as discussed in section 2. In the study, hail events had such an average as followings: Area, 181 km^2; Volume 2, 763 km^3; and mass 798 kTons. For a rainstorm, it valued around 26 km^2, 88 km^3 and 61 kTons, respectively. Meanwhile, overall features of the storms with hail and the frequency distribution, of both months, were significantly higher values than no-hail events. More, the extra statistical analysis could be viewed in Fig. 7.

3.2.5. Echo-top height

The storm echo-top suggested the maximum of radar reflectivity, considered the threshold. In this study, the minimum reflection was set to 30 dBZ as referred to Dixon (1998). Therefore, radar would report only the tops that value from 30 dBZ or higher. For hail reflection, the maximum average of echo-top was higher than the no-hail group in all phases of the study. Fig. 8 shows several frequencies of echo due to hail in the high altitude of 7 to 10 km. Still, no-hail storms were observed most often at altitude of 4 to 5 km.

3.3. Case study of radar signatures during hailstorms on 27 April 2012

The case study focused on exploring the additional radar signature to determine the proper conditions that carry the creation of hail in northern Thailand on 27 April 2012 (in case of HS#3 in Table 1). The purpose of this case study is to illustrate mentioned advantages of polarimetric radar measurements at S band for the case of hail event in northern Thailand. In addition, SIDPOL Radar (Simultaneous Dual Polarization) with EDGE^{TM} Software was also used to measure the main features, such as maximum ZH, Echo-top (ETOP), vertically integrated liquid (VIL), differential reflectivity (ZDR), correlation coefficient (CC), specific differential phase (KDP) and hail probability (HAIL PROB) (Johns *et al*., 1992; Witt *et al*., 1998) (Fig. 9). As regards preliminary signature analysis, at 0918 UTC on 27 April 2012, SIDPOL radar site recorded hailstorms and kept track of these values a warning sign, as shown in Fig. 10. The radar analysis found that it delivered consistent results in case of hail size about 1 to 5cm diameter. Installed at Chiang Muan (Fig. 1), radar site has its sweep radius surrounding about 200 km.

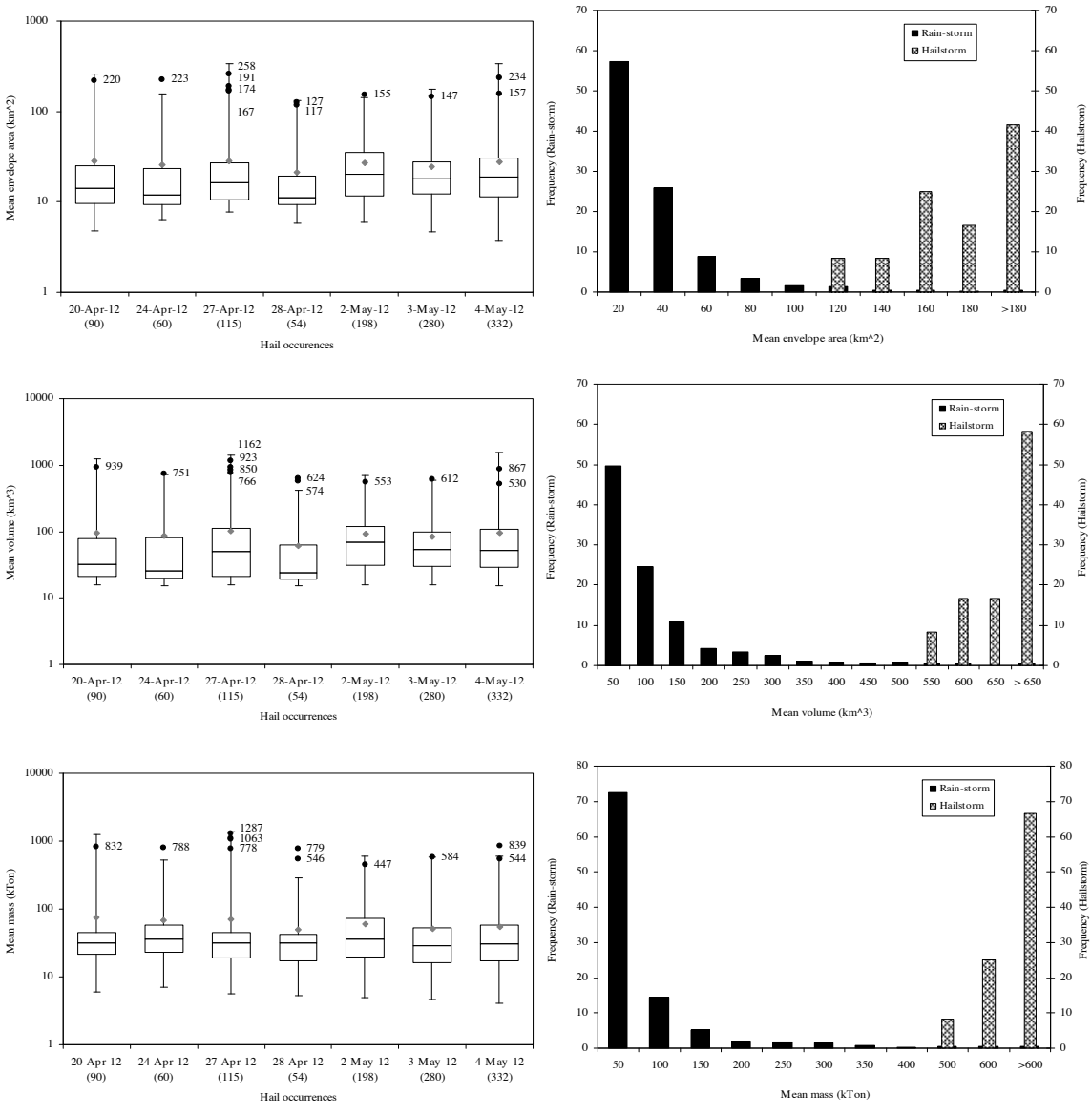

Figure 7. Box and whisker plot of storm's area (km^2), cell volume (km^3) and mass (kTons) (left), number of individual rainstorm incidents each day (in brackets), rainstorms (gray dots), hailstorms (black dots), and frequency distribution (right) during hailstorm.

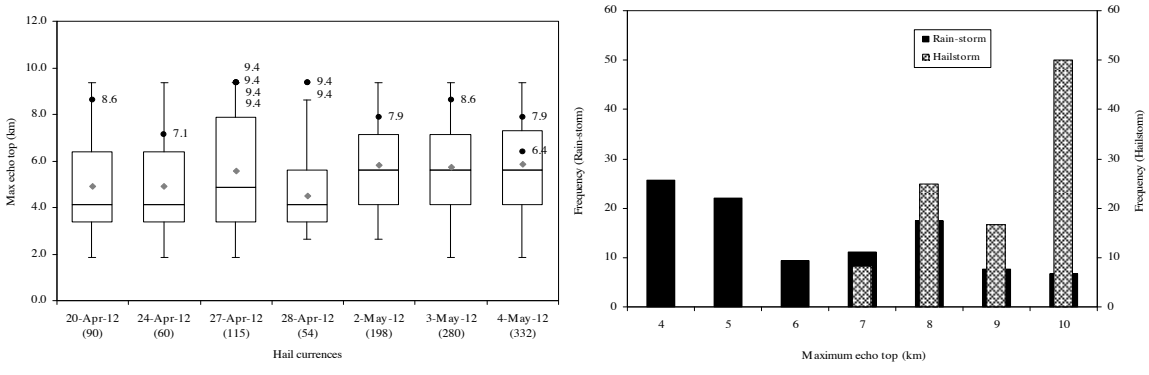

Figure 8. Box and whisker plot of storm echo-top (km) (left), number of individual rainstorm events each day (in brackets), rainstorm (gray dots), hailstorm (black dots), and frequency distribution (right) during hailstorms.

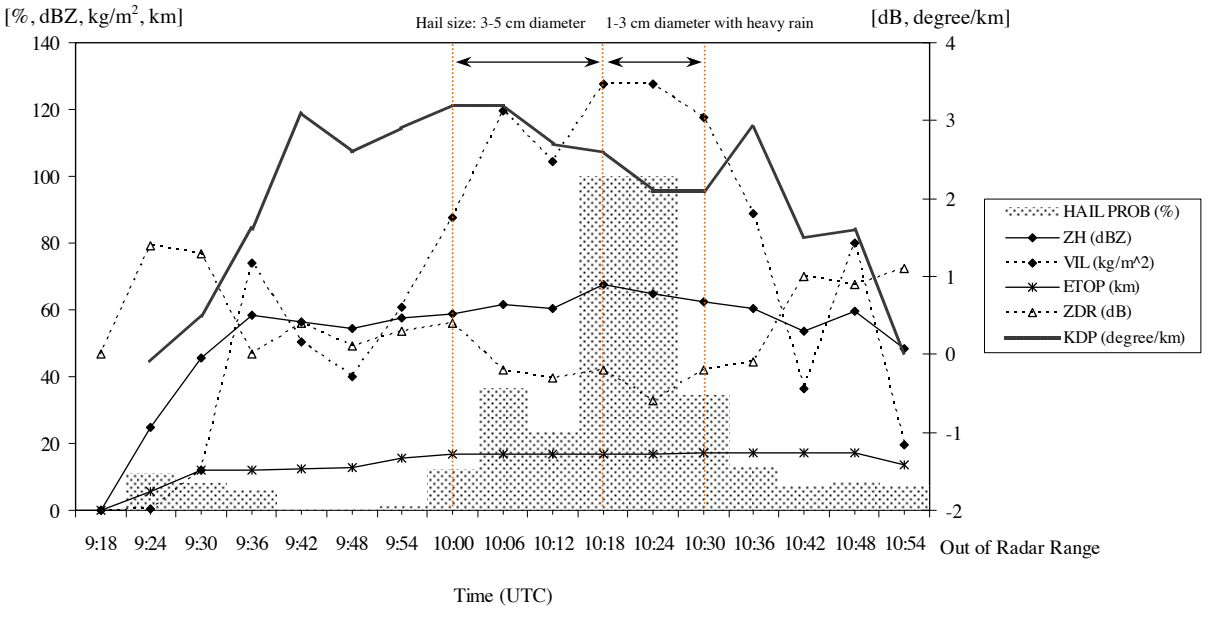

Figure 9. Radar echo structure of hailstorm on 27 April 2012, observation made since no-echo until objects moving far off its radius, and its detection including the maximum value of HAIL PROB (%), ZH, ZDR and VIL (kg/m^2) from 2 km-CAPPI (dBZ), ETOP (km) and KDP (degree/km) at 0. 45^o PPI.

At 1000UTC on 27 April 2012, the severe weather initiated with strong wind and 3-5cm diameter hail size. At 1018 to 1030UTC, 1-3cm hailstones occurred with heavy rain as Fig. 1 shown. As a result, Figs. 9 and 10 suggested as followings (Daniel, 2007).

(1) The values of VIL as high as 120 kg/m^2 between 1000 and 1018 UTC and approached to the highest 128 kg/m^2 at between 1018 and 1024UTC. As agreement with Edwards *et al*. (1998), who studied the correspondence between hailstone size and VIL contents using WSR-88 D in USA, suggested that the severe weathers with VIL as high as 68 kg/m^2 was characterized a sufficient amount of liquid water for hail formation. Accordingly, the result of HAIL PROB exhibited the significant value at 100% between 1012 to 1030UTC consistently with VIL variation.

(2) During hail occurring, the storm revealed a large ZH (> 60 dBZ) according to Houze (1990) represented that ZH > 60 dBZ are likely to occur hail events. ETOP as determined the threshold at 8 dBZ was greater than 17 km. The ZDR approached near zero and fluctuated approximately between -0.6 and 0.5 dB. These were consistent with previous study of (e.g. Aydin *et al*., 1990; Bringi *et al*., 1984; 1986; Illingworth *et al*., 1986) who explained that regions containing ice particles are usually characterized by lower values of ZDR.

(3) The CC is a measure of de-correlation of hydrometeors within a volume. During the hail fall the CC revealed the value between 0.988 and 0.996. From Fig. 10(a)-(f), it exhibited the area of the maximum CC increased, as well as size of hailstones, and occurred approximately 10 km above freezing level (Angela *et al*., 2005).

(4) The KDP values are highest where this phase shift occurs. Hence, high values of KDP indicate areas of heavy rainfall with more liquid precipitation. For this case dealing with hail occurrence, KDP at lowest elevation angle (0.45^o) becomes quite noisy signal from the larger distances away from radar, however; the maximum KDP can vary between 2.1 and 3.2deg/km. It was consistently with previous study of Smyth *et al*. (1999) showed that KDP was exceeding zero and varied with increasing diameter for wet hailstones.

4. Conclusions

The study presented the physical character of summer hailstorms, all 2012-twelve incidents, which occurred in uppermost Thailand. Derived from the upper-air observation through radiosonde, all 18 parameters considerably supported the chances of severe weather startup. All storm properties and products were processed with TITAN and EDGE^{TM}. The results are shown briefly below.

1) The significant parameters for predicting severe weather related to the events of hail and no-hail that comes with the storm include LI, SI and CAPE. These dominance values were found from the thermodynamic analysis where hail was characterized exceeding its average in both April and May 2012. The high negative both LI and SI were presented in marginally instability range of -1 to -4. They were noticeable when the events

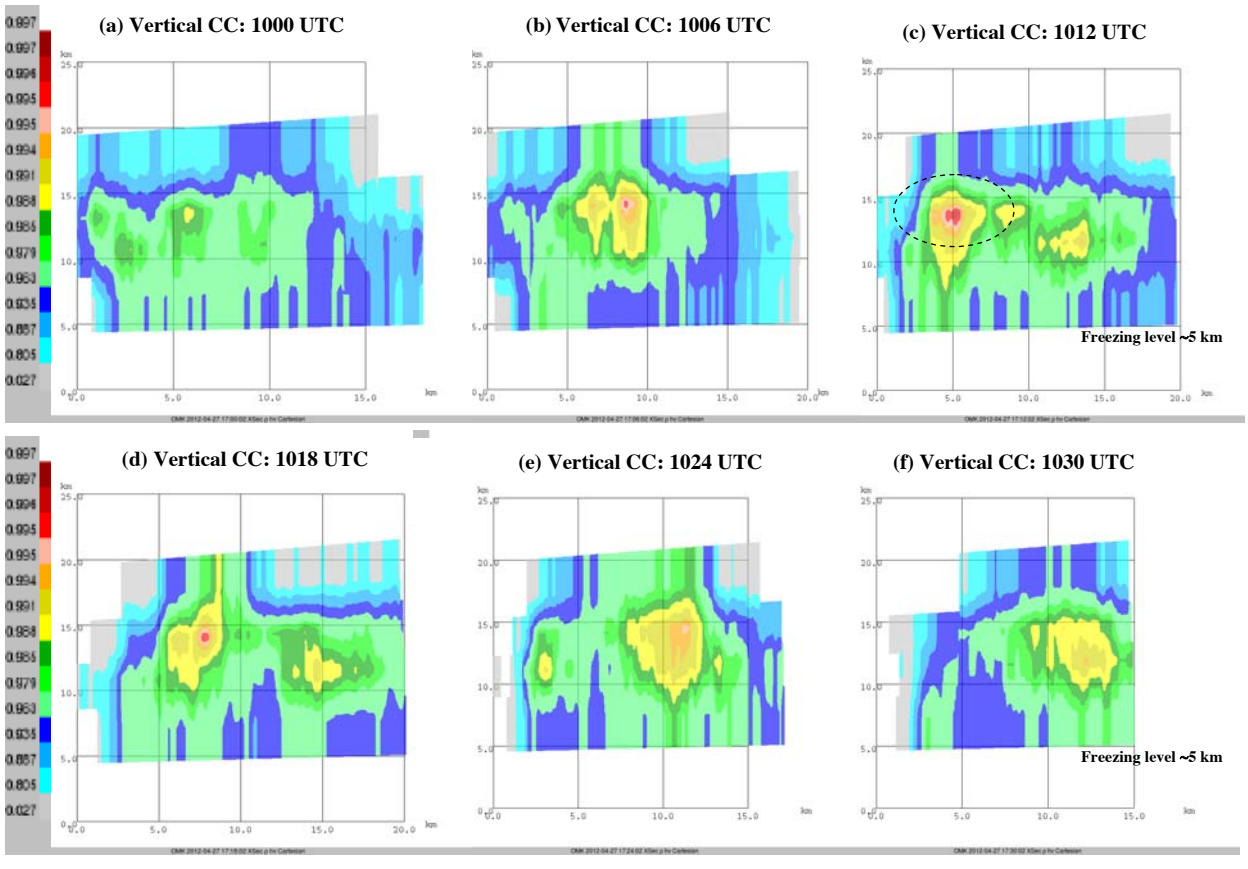

Figure 10. Hailstorm properties of the vertical profile of CC on 27 April 2012 as the 2 km-CAPPI at 1018UTC (a)-(f) varied with time and revealed the maxima at 1012 UTC above freezing level.

occurred during the months. The high value of CAPE reached the extreme instability (CAPE > 2500 J/kg) and related to the large updraft speed. Actual data are in agreement with the knowledge in the air parcel theory. It revealed that hailstorms require the strong updraft to assist hail formation and growth so that it is heavy enough to fall on the ground.

2) Rainstorms and hailstorms were checked with significant 7 storm characteristics that were derived from TITAN. In comparison of their features, the statistical issues included storm duration, speed, mean-maximum reflectivity, area, volume and mass in the dataset. The frequency distribution of storm characteristics showed the scope and limits, together with integrated view of storm's behavior over the monitored area. It was apparent that summer hailstorms had all more greater values than the individual rainstorm. They consisted of storm duration, areas, volume, mass, speed and maximum reflectivity. However, the mean reflectivity of the storm was not helpful in storm identification.

3) With dual polarization, radar was useful for diagnosis to find the severe convective storm on 27 April 2012. Entering into its echo area in Chiang Muan, upper Thailand, and the storm caused severe hail. The result of radar signatures illustrated that during hailfall the probability of hail detection was 100%, VIL was greater than 100 kg/m^2 and ZH revealed the maximum reflectivity larger than 60dBZ near the surface. The ZDR value of rain-hail mixtures could be near zero. ETOP was greater than 17 km as determined threshold at 8dBZ, the CC revealed the value between 0.988 and 0.996 and the KDP exhibited the values between 2.1 and 3.2 deg/km.

5. Limitations of study and implications for operational weather forecasting

The analysis was performed under the limitation of all 12 hailfall events in two months of the 2012 summer. Besides, it had the restriction on areas that were defined in Omkoi, Chiangmai, covering all areas for inspection with SIDPOL radar. Hence, the number of hail-birth would be considered since the hail occurred infrequently. The quantitative estimate of hailstorms could not be done due to considered variables serving dissimilar role. The analysis result, as well as the future study and research, might be applied easily and correctly if those parameters are monitored to find the period supporting the certain event or backing extreme

events in the context of the climatology. This enables us to predict possible severe weather.

Acknowledgements

The authors gratefully acknowledge the Department of Royal Rainmaking and Agricultural Aviation (DRRAA), Bangkok Thailand for funding support through BRRAA research project 2012: forecasting model development using upper atmospheric weather observation in northern Thailand (NTCM project). We also appreciate the Research Group and the Royal-Rainmaking Atmospheric Observation Group for providing the radar data sets and weather observation data used in this study. We would thank to all staff at Omkoi weather station and Huahin research center for much helpfulness in data collection and processing. Last, we express our thankful to Mr.Asadarndej Pokam and Mr.Rod Phillips for their invaluable assistance.

References

Angela R, Pamela LH, Schuur T. Estimating hail size using polarimetric radar. Fourth AMS Student Conference 2005.

Aydin K, Zhao Y, Seliga TA. A differential reflectivity radar hail measurement technique: Observations during the Denver hailstorm of 13 June 1984. Journal of Atmospheric and Oceanic Technology 1990; 7: 104-13.

Barnes SL. Report on a meeting to establish a common Doppler radar data exchange format. Bulletin of the American Meteorological Society 1980; 61(11): 1401-04.

Battan LJ. Relationship between cloud base and initial radar echo. Journal of Applied Meteorology 1963; 2: 333-36.

Braham RR. Cumulus cloud precipitation as revealed by RADAR-ARIZONA 1955. Journal of Meteorology 1958; 15: 75-83.

Brimelow JC, Reuter GW, Poolman ER. Modeling maximum hail size in Alberta thunderstorms. Weather and Forecating 2002; 17: 1048-62.

Bringi VN, Seliga TA, Aydin K. Hail detection with a differential reflectivity radar. Science 1984; 225(4667): 1145-47.

Bringi VN, Vivekanandan J, Tuttle JD. Multiparameter radar measurements in Colorado convective storms. Part II: Hail detection studies. Journal of the Atmospheric Sciences 1986; 43(22): 2564-77.

Bringi VN, Chandrasekar V. Polarimetric Doppler weather radar. Cambridge University Press, UK. 2001.

Browning KA. The structure and mechanism of hailstorms. Meteorological Monographs 1977; 16: 1-39.

Ceperuelo M, Llasat MC, López L, García-Ortega E, Sánchez JL. Study of 11 September 2004 hailstorm event using radar identification of 2-D systems and 3-D cells. Advances in Geosciences 2006; 7: 215-22.

Changnon SA. Twenty-five most severe summer hailstorms in Illinois during 1915-1959: Research report No. 4. Crop-Hail Insurance Actuarial Association, Chicago, Ill. USA. 1960.

Changnon SA. Monthly and semi-monthly distributions of hail days in Illinois: Research report No. 17. Crop-Hail Insurance Acturial Association, Chicago, Ill. USA. 1963.

Changnon SA. Hail evaluation techniques part 1 final report, Contract No. NSF GA-482. State Water Survey, Urbana, Ill, USA. 1969.

Changnon SA, Changnon D, Hilberg SD. Hailstorms across the nation: An atlas about hail and its damages. Illinois State Water Survey Contract Report 2009-12, USA. 2009; 1-92.

Chantraket P, Detyothin C, Suknarin A. Radar reflectivity derived rain-storm characteristics over Northern Thailand. EnvironmentAsia 2013; 6(2): 24-33.

Daniel CH. Case study of the record hail event and severe thunderstorm outbreak in East-Central Nebraska on 22-23 June 2003. Mesoscale Meteorology (AOS 453) 2007; 3: 1-17.

Debin S, Jianli M, Qiang Z, Daren L. A preliminary study of hail identification with X-Band dual polarization radar. The sixth european conference on radar conference on radar in meteorology and hydrology - ERAD. 2010.

Delobbe I, Holleman I. Radar-based hail detection: Impact of height assignment errors on the measured vertical profiles of reflectivity. In Preprints 31at Conference on Radar Meteorology. American Meteorology Society. 2003; 475-78.

Dixon M, Wiener G. TITAN (Thunderstorm Identification, Tracking, Analysis, and Nowcasting) - A radar-based methodology. Journal of Atmospheric and Oceanic Technology 1993; 10(6): 785-97.

Dixon M. Report on preliminary radar based analysis of seeding effects. Coahuila Rainfall Argumentation Program 1997/1998 Seasons, NCAR, USA. 1998; 1-7.

Doswell CAIII, Rasmussen EN. The effect of neglecting the virtual temperature correction on CAPE calculations. Weather and Forecasting 1994; 9: 625-29.

Edwards R, Thompson RL. Nationwide comparisons of hail size with WSR- 88D vertically liquid integrated water and derived thermodynamic sounding data. Weather and Forecasting 1998; 13(2): 277-85.

Groenemeijer PH, Delden AV. Sounding-derived parameters associated with large hail and tornadoes in the Natherlands. Atmospheric Research 2007; 83(2-4): 473-87.

Hohl R, Schiesser HH, Aller D. Hailfall: The relationship between hail kinetic energy and hail damage to buildings. Atmospheric Research 2002; 63(3-4): 177-207.

Höller H. Mesoscale organization and hailfall characteristics of deep convective in southern Germany. Beitraege zur Physik der Atmosphaere 1994; 67(3): 219-34.

Houze RA, Rutledge SA, Biggerstaff MI, Smull BF. Interpretation of Doppler weather radar displays of midlatitude mesoscale convective system. Bulletin American Meteorological Society 1989; 70(6): 608-19.

Illingworth AJ, Goddard JWF, Cherry SM. Detection of hail by dual-polarization radar. Nature 1986; 320: 431-33.

Johns RH, Doswell CAIII. Severe local storms forecasting. Weather Forecasting 1992; 7: 588-612.

Knight CA, Knight NC. Hailstorms. Meteorological Monographs 2001; 28: 223-48.

Lim S, Chandrasekar V, Bringi VN. Hydrometeor classification system using dual-polarization radar measurements: model improvements and in-situ verification. IEEE Transaction on Geoscience and Remote Sensing 2005; 43(4): 792-801.

Ludlam FH. Clouds and storms: The behavior and effect of water in the atmosphere. Pennsylvania State University Press, USA. 1980.

Miller LJ, Tuttle JD, Knight CA. Airflow and hail growth in a severe northern high plains supercell. Journal of the Atmospheric Sciences. 1988; 45(4): 736-62.

Nelson SP. The hybrid multicellular-supercellular storm: An efficient hail producer. part II: General characteristics and implication for hail growth. Journal of the Atmospheric Sciences 1987; 44(15): 2060-73.

Ragette G. Mesoscale circulations associated with Alberta hailstorms. Monthly Weather Review 1973; 101(2): 150-59.

Robert JG. Analysis of stability indices for severe thunderstorms in the Northeastern United States. Honors Thesis Presented to the College of Agriculture and Life Sciences. Physical Sciences of Cornell University, USA, 2009.

Roxana DC, Sorin B, Roxana B, Alexandru D. Assessment of the destructive potential of hail. Geophysical Research 2013; 15(EGU): 2013-9653.

Sanchez JL, López L, Gil-Robles B, Dessens J, Bustos C, Berthet C. Short -term forecast of hail precipitation parameters. 5th European Conference on Severe Storms 12-16 October 2009.

Smyth TJ, Blackman TM, Illingworth AJ. Observations of oblate hail using dual polarization radar and implications for hail-detection schemes. Quarterly Journal of the Royal Meteorological Society 1999; 125: 993-1016.

Straka JM, Zrnic DS, Ryzhkov AV. Bulk hydrometeor classification and quantification using polarimetric radar data: synthesis of relations. Journal of Applied Meteorology and Climatology 2000; 39: 1341-72.

Towery NG, Changnon SA. Characteristics of hail-producing radar echoes in Illinois. Monthly Weather Review 1970; 98(5): 346-53.

Vivekanandan J, Zrnic DS, Ellis SM, Oye R, Ryzhkov AV, Straka J. Cloud microphysics retrieval using S-band dual-polarization radar measurements. Bulletin of the American Meteorological Society 1999; 80(3): 381-88.

Vulpiani G, Marzano FS, Chandrasekar V, Lim S. Constrained iterative technique with embedded neural-network for dual-polarization radar correction of rain path attenuation. IEEE Transaction and Remote and Sensing 2005; 43(10): 2305-14.

Witt A. A hail core aloft detection algorithm. Preprints, 16th Conference on Severe Local Storms, American Meteorological Society 1990; 256-59.

Witt A, Eilts DM, Stumpf JG, Johnson JT, Mitchell ED, Thomas WK. An enhanced hail detection algorithm for the WSR-88D. Weather and Forecasting 1998; 13: 286-303.

Waldvogel A, Federer B, Grimm P. Criteria for the detection of hail cells. Journal of Applied Meteorology 1979; 18(12): 1521-25.

Xie B, Zhang Q, Wang Y. Observed characteristics of hail size in four regions in China during 1980-2005. Journal of Climate, 2010; 23: 4973-81.

Zrnic DS, Ryzhkov A, Straka J, Liu Y, Vivekanandan J. Testing a procedure for automatic classification of hydrometeor types. Journal of Atmospheric and Oceanic Technology 2001; 18: 892-913.

Received 12 September 2014
Accepted 5 November 2014

Correspondence to
Pakdee Chantraket
Department of Royal Rain-making and Agricultural Aviation (DRRAA),
Bangkok 10900,
Thailand
E-mail: pakdee2@hotmail.com